

# Classical Heisenberg antiferromagnet on a garnet lattice: A Monte Carlo simulation

O. A. Petrenko<sup>1,2</sup> and D. McK. Paul<sup>2</sup>

<sup>1</sup>ISIS Facility, Rutherford Appleton Laboratory, Chilton, Didcot, OX11 0QX, United Kingdom

<sup>2</sup>University of Warwick, Department of Physics, Coventry, CV4 7AL, United Kingdom

(Received 27 September 1999; revised manuscript received 22 August 2000; published 15 December 2000)

We have studied a classical antiferromagnet on a garnet lattice by means of Monte Carlo simulations in an attempt to examine the role of geometrical frustration in gadolinium gallium garnet  $\text{Gd}_3\text{Ga}_5\text{O}_{12}$  (GGG). Low-temperature specific heat, magnetization, susceptibility, the autocorrelation function  $A(t)$ , and the neutron scattering function  $S(Q)$  have been calculated for several models including different types of magnetic interactions and with the presence of an external magnetic field applied along the principal symmetry axes. A model, which includes only nearest-neighbor exchange  $J_1$ , neither orders down to the lowest temperature nor does it show any tendency towards forming a short-range coplanar spin structure. This model, however, does demonstrate a magnetic field induced ordering below  $T \sim 0.01J_1$ . In order to reproduce the experimentally observed properties of GGG, the simulated model must include nearest-neighbor exchange interactions and also dipolar forces. The presence of weak next-to-nearest exchange interactions is found to be insignificant. In zero field  $S(Q)$  exhibits diffuse magnetic scattering around positions in reciprocal space where antiferromagnetic Bragg peaks appear in an applied magnetic field.

DOI: 10.1103/PhysRevB.63.024409

PACS number(s): 75.40.Mg, 75.50.Ee

## I. INTRODUCTION

The introduction of frustration to magnetic systems leads to extra degeneracy for the ground state in addition to the degeneracy resulting from the symmetry of magnetic Hamiltonian. The larger this additional degeneracy, the more likely frustration is to cause dramatic changes in the magnetic properties of the system, such as the absence of long range order even at the lowest temperature. Geometrical frustration has been one of the key issues in magnetism for at least twenty years. A recent wave of theoretical papers<sup>1,2</sup> as well as publications dealing with Monte Carlo simulation<sup>3-6</sup> has emphasized the unusual magnetic properties of geometrically frustrated systems. The question of whether the frustration leads to a disordered gapped state or to long-range Néel type order in different types of geometry is still under debate. Current efforts seem to be concentrated around two types of lattices: the *kagomé* lattice<sup>2,5,7</sup> and the pyrochlore lattice.<sup>1,3</sup> Recently has it been established that the pyrochlore lattice represents the only simple system for which the additional degree of freedom caused by the frustration is extensive—it is proportional to the number of spins involved.<sup>8</sup>

The growth of theoretical interest in the pyrochlore lattice, a lattice of corner-sharing tetrahedra, is driven largely by experimental discoveries.<sup>9</sup> There are many chemically clean pyrochlores (some of which may be produced as single crystals<sup>10</sup>) with different types of magnetic atoms and interactions, which allows one to pick the most suitable one for study and for comparison with a particular theoretical model. By studying the phenomenon in general a much better understanding of the magnetic properties of individual compounds can be achieved. The same reasoning applies to another geometrically frustrated system—an antiferromagnet on a *kagomé* lattice, where  $\text{SrCr}_9\text{Ga}_{12-9p}\text{O}_{19}$ ,<sup>11</sup> jarosites,<sup>12</sup> and some other compounds<sup>13</sup> provide quite a variety of model systems.

Gadolinium gallium garnet,  $\text{Gd}_3\text{Ga}_5\text{O}_{12}$ , is a *unique* ex-

ample of an antiferromagnet on the garnet lattice. There are no other compounds matching its magnetic properties. In GGG (space group  $Ia\bar{3}d$ ) the magnetic Gd ions are located on two interpenetrating, corner-sharing triangular sublattices, where the triangles of spins do not lie in the same plane—the angle between two nearest triangles is equal to the angle between the diagonals of a cube,  $70.5^\circ$  (see Fig. 1). In this compound the triangular arrangement of the nearest spins is combined with complete exchange isotropy (the single-ion anisotropy is negligibly small<sup>14</sup>) and with a relatively strong dipole-dipole energy. Although the magnetic properties of various garnets have been thoroughly studied during the past half century, the analogy between any of them and GGG is not straightforward. All other magnetic garnets order at some low temperature, while GGG does not. No long range magnetic order has been detected in GGG down to 25 mK,<sup>15</sup>

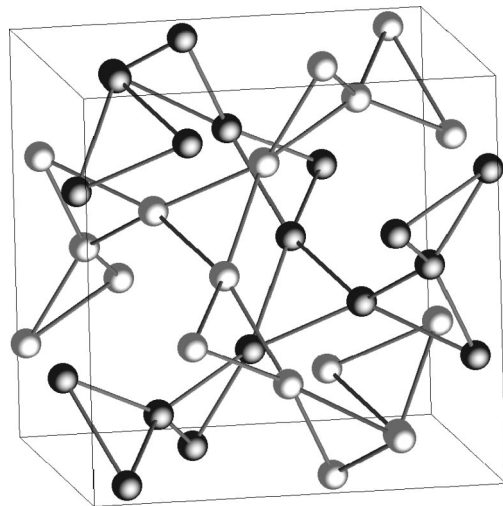


FIG. 1. Positions of the magnetic Gd ions in a garnet structure. There are 24 magnetic ions per unit cell, they are divided into two interpenetrating sublattices.

while other gallium garnets based on Dy, Nd, Sm, and Er, rather than Gd, have been found to be magnetically ordered at temperatures below 1 K.<sup>16</sup> The nearest analogy to GGG would probably be found among the Mn-based garnets, where the single-ion anisotropy is also very small. However two similar magnetically isotropic garnets  $\text{Mn}_3\text{Al}_2\text{Ge}_3\text{O}_{12}$  and  $\text{Mn}_3\text{Al}_2\text{Si}_3\text{O}_{12}$ ,<sup>17</sup> also order. Most likely this is due to the presence of relatively strong next-to-nearest exchange interactions. If and when the degeneracy of the ground state is removed and the system undergoes a phase transition to a long-range ordered state, almost all complications disappear. The magnetic ground state and the main interactions are known from experiment and theoretical calculations are straightforward. Numerical estimates exist to at least the accuracy that experiments currently attain. However, a theoretical model describing adequately the magnetic properties of GGG still has to be developed.

This paper presents the results of classical Monte Carlo simulations of the magnetic properties of the Heisenberg antiferromagnet on a garnet lattice. While some of the initial results related to the GGG have been briefly reported in our neutron scattering papers,<sup>18,19</sup> where they have been used to explain the obtained experimental data and also to predict possible experiments, here we take a more general approach to the problem. We address issues which are not necessarily directly related to GGG, but are interesting from a theoretical point of view, e.g., we discuss properties of a model which includes nearest-neighbor exchange interactions only. Where possible we compare with the results of simulations for the pyrochlore and *kagomé* lattices and show, that an antiferromagnet on a garnet lattice is yet another highly frustrated magnetic system exhibiting a number of unusual and intriguing properties.

## II. SIMULATION MODELS

We consider the Hamiltonian

$$\hat{\mathcal{H}} = \sum_{\langle i,j \rangle} J_{ij} \mathbf{S}_i \mathbf{S}_j + D \sum_{\langle i,j \rangle} \left[ \frac{\mathbf{S}_i \mathbf{S}_j}{r_{ij}^3} - 3 \frac{(\mathbf{S}_i \mathbf{r}_{ij})(\mathbf{S}_j \mathbf{r}_{ij})}{r_{ij}^5} \right], \quad (1)$$

where the spins  $\mathbf{S}_i$  are classical, three-component vectors on the  $\text{Gd}^{3+}$  sites of a garnet lattice,  $S = 7/2$  as in GGG. The first term is the exchange interaction, the second term is the dipole-dipole interaction between the magnetic moments.

The original idea to simulate the magnetic properties of GGG using MC methods belongs to Kinney and Wolf,<sup>20</sup> who calculated the temperature dependence of the specific heat and by comparing the results with the experimental data have obtained the amplitudes of the nearest- and next-nearest-neighbor exchange interactions  $J_1$ ,  $J_2$ , and  $J_3$ . More recently Schiffer *et al.* calculated the magnetic phase boundary and have investigated the magnetic structure of GGG in an applied field.<sup>21</sup> We use the same value of the nearest exchange constant as Kinney and Wolf,<sup>20</sup>  $J_1 = 0.107$  K, because it produces good estimates for the temperature dependence of the susceptibility and also for the saturation field of the magnetization.<sup>22</sup> However, as will be shown later, the values of  $J_2$  and  $J_3$  quoted in Ref. 20 are not essential: as

long as they are small in comparison with  $J_1$ , they do not change significantly the predicted magnetic properties of GGG and therefore can not be reliably determined from the MC simulations.

The strength of the dipole-dipole interaction  $D$  is defined by the distances between the  $i$ th and  $j$ th spins. In GGG the  $\text{Gd}^{3+}$  sites are separated by  $(\sqrt{6}/8)a = 3.781$  Å, where  $a = 12.349$  Å is the lattice constant at low temperature. Therefore we use  $D_{dd} = 0.0457$  K for the strength of the nearest-neighbor dipolar interaction. It is very important and at the same time very difficult to simulate reliably such a long range interaction as the dipole-dipole one. For some simpler lattices, for example, a 2D-square lattice,<sup>23</sup> or for highly anisotropic systems, such as *spin ice* pyrochlores,<sup>24</sup> the Ewald summation technique can be used to treat the long-range nature of the dipole-dipole interaction. In case of Heisenberg spins located on the complicated lattice of GGG, however, there is no option but to introduce a cut-off range  $R_0$  and to neglect the dipole-dipole interaction for all distances larger than  $R_0$ . Previous simulations have restricted the dipole-dipole interaction to a third neighbor,<sup>20,21</sup> while in our model  $R_0$  has been extended to include the fourth neighbor. We have also made several test runs to compare the simulation results for this model with both shorter (to a third neighbor) and also longer (ten neighbors) cutoff ranges and have found no significant difference, which suggests that this model describes the dipolar force reasonably well. The dipolar interaction between two magnetic moments decays as  $1/R^3$ , the number of neighbors in a shell  $\delta R$  is proportional to  $R^2$ , therefore the dipole-dipole energy should decay only relatively slowly, as  $1/R$ . In reality, however, the extension of the cutoff range from a third neighbor to a fourth one does not change significantly either the total dipolar energy, nor the overall system energy. A possible answer to this puzzle might be related to the fact that all magnetic interactions in GGG, including the dipolar one, are frustrated: the contribution of the individual magnetic moments to the total system energy is mutually cancelled or nearly cancelled, therefore for each magnetic moment only the local surroundings influence the choice of magnetic orientation. Similar observations have been made during recent Monte Carlo simulations on pyrochlorelattice which included long-ranged dipole-dipole as well as short-ranged exchange interactions.<sup>4</sup>

MC simulations have been performed for lattice sizes  $L \times L \times L$ , with  $L = 3$  to 9 unit cells, containing 648 to 17 496 spins. Significantly larger lattice sizes, than previously used, have ensured that the magnetic correlation length in the disordered phase does not exceed the system size. Simulations with larger lattice sizes have improved the resolution of the calculated scattering function  $S(Q)$ , in an applied magnetic field allowing us to resolve clearly individual magnetic Bragg peaks. A standard Metropolis algorithm with periodic or open boundary condition has been employed; up to several millions Monte Carlo steps per spin (MCS) were performed at the lowest temperatures. Where possible an attenuation factor  $\delta S$  has been introduced in such a way that roughly 50% of the attempted spin moves were accepted,<sup>25</sup> which has resulted in a dramatic increase of the spin relaxation rate. For the simulations in a magnetic field this proce-

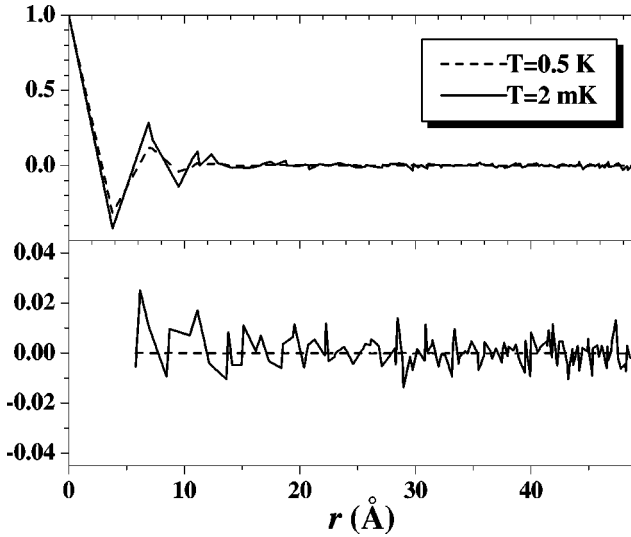


FIG. 2. Correlation function for a system of  $5 \times 5 \times 5$  unit cell sizes (3000 spins), which includes only nearest-neighbor exchange interaction  $J_1$ . Top: the correlation between spins belonging to the same sublattice, bottom: correlation between sublattices.

ture has been abandoned to permit the system to make abrupt structural changes. The magnetic field is assumed to be applied along the (100) direction unless otherwise stated.

### III. RESULTS AND DISCUSSION

#### A. Zero external field properties

We begin by addressing the issue of the phase transition at low temperature in zero magnetic field. In GGG no sign of long range magnetic order has been found down to 25 mK,<sup>15</sup> moreover, frustration induced spin freezing has been suggested at temperatures below 125–135 mK on the basis of single crystal magnetization measurements: the susceptibility is frequency dependent, and the static magnetization is different for field cooling and zero field cooling.<sup>26</sup> However, neutron scattering experiments show that at the lowest temperatures the magnetic system is not frozen completely.<sup>18</sup> It rather behaves as a mixture of a liquid and solid states.

The first thing to notice is that the simulation model, which includes only nearest-neighbor exchange  $J_1$  does not show any sign of a phase transition down to at least  $T = 1$  mK (which is less than 0.1% of the exchange energy  $JS^2$ ). Several measured quantities show that the system remains in a spin-liquid (or, following Villain,<sup>27</sup> a cooperative paramagnet) phase: averaging over sufficiently long time gives zero magnetic moment on each site, the scattering function  $S(Q)$  does not show any sharp peaks, the magnetic correlation length  $Q(r) \equiv \langle \mathbf{S}(0) \cdot \mathbf{S}(r) \rangle$  does not exceed the system size (see Fig. 2). In fact, close inspection of Fig. 2 reveals that correlations are very small beyond the first unit cell. In addition there is no obvious maximum or cusp in the heat capacity temperature dependence (see Fig. 3). To test the suspicion that at low-temperature Monte Carlo simulations are not effective enough in allowing the system to reach equilibrium, we have checked whether the simulation results depend upon the starting conditions. No difference in

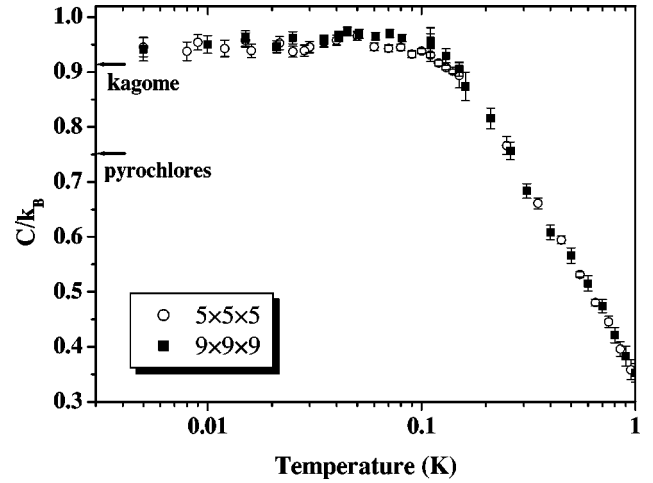


FIG. 3. Specific heat temperature dependence for an open boundary conditions model of  $5 \times 5 \times 5$  and  $9 \times 9 \times 9$  sizes which includes only the nearest-neighbor exchange interaction  $J_1$ . Up to  $4 \times 10^6$  MCS have been performed at lower temperatures.

results have been noticed when starting calculations from an initially random or a  $120^\circ$  planar triangular state.

The low-temperature specific heat itself is an important thermodynamic quantity, whose value is sensitive to the presence of zero modes<sup>6</sup> and quartic modes.<sup>8</sup> In the pyrochlore lattice each quadratic mode contributes  $k_B/2$  to the heat capacity, each quartic mode  $k_B/4$  and zero modes do not contribute at all, thus reducing the zero-temperature specific heat to  $3k_B/4$ ,<sup>8</sup> while in *kagomé* lattice it is reduced to  $11k_B/12$ .<sup>6</sup> Our initial calculation on a relatively small system with periodic boundary conditions showed that  $C(T=0)$  was indistinguishable from unity within the accuracy of the simulations. However, prompted by the comparison with the *kagomé* and pyrochlore lattice results, we have performed much longer Monte Carlo runs on much bigger systems with open boundary conditions (we use open boundary conditions in order to avoid the imposition of periodicity on a potentially incommensurate magnetic system). As can be seen from Fig. 3,  $C(T=0) \approx 0.94(2)$  with the accuracy of the calculation sufficiently high to claim that it is actually below unity. There is no significant difference in  $C(T=0)$  calculated for systems of  $5 \times 5 \times 5$  and  $9 \times 9 \times 9$  containing 3000 and 17 496 spins, respectively.

The introduction of the dipolar interactions slows down the spin-relaxation process. Figure 4 displays the time dependence (time is measured in MCS) of the autocorrelation function  $A(t) = (1/N) \sum \langle \mathbf{S}_i(0) \mathbf{S}_i(t) \rangle$  for the two models: with (bottom) and without (top) dipolar forces. The model which includes dipole-dipole interactions does not show noticeable relaxation by  $T = 50$  mK, while the model with only nearest exchange interactions is still relaxing even at an order of magnitude lower temperature. The difference between the autocorrelation function for these two models is evident at all temperatures below 0.5 K, which approximately coincides with the nearest-neighbor dipolar energy  $D_{dd} \times S^2$ .

Dealing with very slow relaxing spin systems and a potential spin-glass transition it is essential to ensure that the simulation time is longer than the equilibration time. In prac-



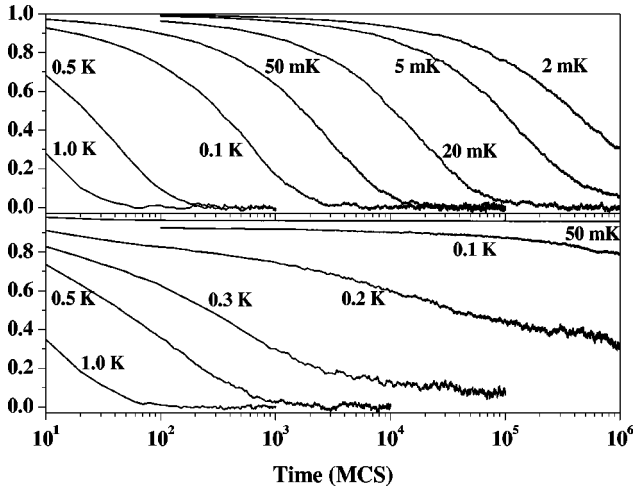


FIG. 4. Time dependence (in Monte Carlo steps per spin) of the autocorrelation function  $1/N\langle S(0)S(t) \rangle$  for various temperature from  $T=1$  K down to 2 mK in a model which includes (a) only the nearest-neighbor exchange interaction  $J_1$  (b) the nearest-neighbor exchange interaction and the dipole-dipole interactions up to fourth neighbor. System with a lattice size  $9 \times 9 \times 9$  unit cells has been used for this calculation.

tice the first  $t_0$  MCS are used only for equilibration and then calculations and averaging are carried out during the next  $t_0$  steps. An estimation of an appropriate value of  $t_0$  could be obtained following the procedure introduced by Bhatt and Young,<sup>28</sup> where the spin-glass susceptibility  $\chi_{SG}$  has been calculated in two different ways. In the first method we calculate an overlap between two uncorrelated sets of spins which approaches  $\chi_{SG}$  from below, if  $t_0$  is shorter than the equilibration time. In the second approach the four-spin-correlation function is calculated, which approaches  $\chi_{SG}$  from above, if  $t_0$  is small. The  $t_0$  is considered to be long enough and the results are accepted only if the two estimates of  $\chi_{SG}$  agreed. In a GGG model which includes both exchange and dipolar interactions  $t_0$  becomes enormously long at low temperatures. In fact even during the runs with  $t_0 = 10^6$  MCS the results showed no agreement between the two approaches for all temperatures below  $T=100$  mK. Therefore the results of calculations in zero field for a model which includes dipole-dipole interactions could not be considered as reliable below this temperature. The problem of long equilibration times is removed by the application of an external magnetic field.

The results of the simulations with the model, which takes into account only the nearest-neighbor exchange interaction  $J_1$  fits well the experimental neutron scattering function  $S_p(Q)$  at all temperatures above 140 mK.<sup>18</sup> The neutron scattering function  $S_p(Q)$  for a powder sample is calculated as

$$S_p(Q) = f(Q)^2 \sum_{i,j} \langle \mathbf{S}_i \mathbf{S}_j \rangle \frac{\sin(Qr)}{Qr}, \quad (2)$$

where  $f(Q)$  is the magnetic form factor.  $S_p(Q)$  has several broad diffuse scattering peaks (see Fig. 5 in Ref. 18), whose intensity increases as the temperature decreases in agreement

with the experiment. The introduction of the dipole-dipole interaction at these temperatures does not change  $S_p(Q)$  significantly.

A somewhat unexpected results have been obtained earlier<sup>29</sup> for a single crystal neutron scattering function, calculated as

$$S_{xt}(Q) = \left( f(Q) \sum_n \mathbf{q}_n e^{i\mathbf{Q}r_n} \right)^2, \quad (3)$$

where  $\mathbf{q}_n$  is the magnetic interaction vector. Even at temperature well above  $T=140$  mK, where there is no problem from very long equilibration times,  $S_{xt}(Q)$  demonstrates a tendency to form incommensurate peaks around integer positions in the reciprocal space (see Fig. 4 in Ref. 29). The intensity of these incommensurate peaks is much lower than the expected intensity of the true long-range order Bragg peaks, and their width is determined by the system size. The exact position of these peaks in reciprocal space is not fixed, it may change from one ‘‘snap shot’’ of  $S_{xt}(Q)$  to another. Only after averaging significantly large amount of the ‘‘snap shots’’ (from several dozens to several hundreds) a clear picture of the short-range incommensurate magnetic order was obtained. However, this is most likely to be an artificial effect caused by the periodic boundary conditions: when they are removed, the effect of splitting seems to disappear. Top panel of Fig. 5 shows simulated single crystal neutron scattering intensity of GGG in the  $(hk0)$  plane at  $T=0.2$  K.

Another interesting aspect of this study is to investigate how the ratio of exchange to dipolar interactions influences properties of the Heisenberg antiferromagnet on a garnet lattice. In GGG  $J_1$  is about twice the strength of  $D_{dd}$  and there is no magnetic order, while in Mn-based garnets<sup>17</sup> the ratio  $J_1/D_{dd}$  is slightly higher and they do order. For instance, in  $\text{Mn}_3\text{Al}_2\text{Ge}_3\text{O}_{12}$ , which undergoes an antiferromagnetic phase transition to a  $120^\circ$  structure at  $T_N=6.65$  K, the  $J_1 = 0.57$  K (Ref. 30) is more than ten times stronger than  $D_{dd}$  in GGG. Our simulation shows that this fact alone could not lead to the appearance of the long-range magnetic order. In a model, where  $J_1$  has been increased up to a hundred times keeping the  $D_{dd}$  value fixed, the ground state remained disordered. However, the introduction of the next-to-nearest exchange interaction with a value cited in Ref. 30,  $J_2 = 0.12$  K, does make a difference: the system immediately undergoes a phase transition to a LRO state, which reveals itself clearly both as a cusp in a heat capacity temperature dependence and as peaks in the scattering function  $S(Q)$ .

## B. Magnetic properties in an applied field

As has been mentioned above, in an applied magnetic field the problem of long equilibration times is much less severe, which gives us an excellent opportunity to investigate the magnetic phase diagram of GGG in detail. A phase transition to a LRO state in magnetic field was detected by calculating the specific heat temperature dependence in constant field or by calculating its field dependence at constant temperature. Figures 4 and 5 in Ref. 19 give examples of such calculations. The position of the specific heat maximum is

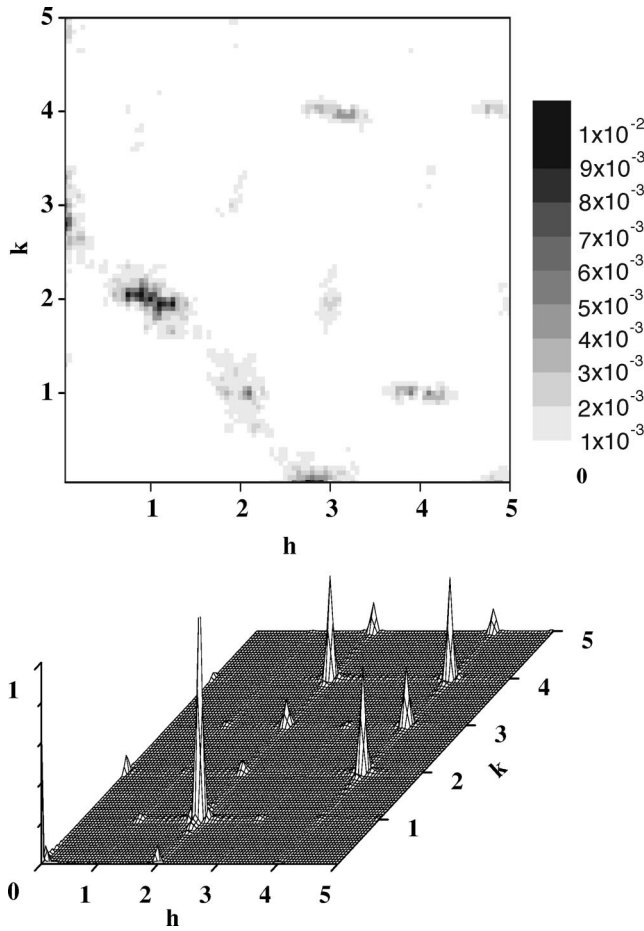


FIG. 5. Simulated single crystal neutron scattering intensity of in the  $(hk0)$  plane at  $T=0.2$  K in a zero field (top panel) and in a field of  $H=1.06$  T applied along  $(001)$  direction (bottom panel). The data have been obtained according to formula (3) for a model size of  $9 \times 9 \times 9$  unit cells with open boundary conditions.

not sensitive to the introduction of the relatively weak next-to-nearest exchange interactions (such as were quoted in Ref. 20,  $J_2 = -0.003$  K and  $J_3 = 0.010$  K), neither does it show any visible size dependence. In the field dependence of the specific heat, only one anomaly corresponding to the upper transition field is well pronounced, while there is no obvious anomaly corresponding to the lower transition field, which agrees with previous MC simulations.<sup>21</sup>

In order to reproduce accurately the experimentally observed phase diagram of GGG, the simulation model must include nearest-neighbor exchange interactions and also dipolar forces. However, even in the model including only nearest-neighbor exchange more accurate calculations revealed signs of the phase transitions in a magnetic field. Figure 6 presents the magnetization curves and also their derivatives at  $T=1$  mK for such models. Before reaching a saturation point at  $H \approx 1.7$  T, the raw magnetization shows a relatively small change of the slope around  $H \approx 0.6$  T, which is not really a striking feature and therefore has passed unnoticed in our earlier calculations. In the susceptibility curves, however, a clear minimum is present at  $H \approx 0.6$  T. We believe that this minimum in susceptibility corresponds

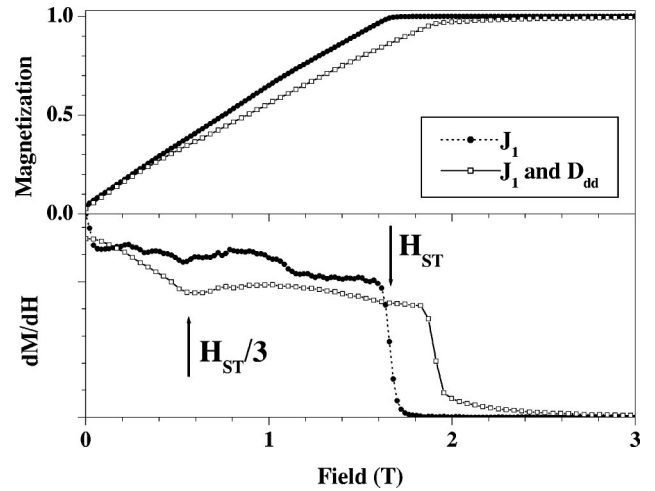


FIG. 6. Field dependence of the magnetization (top) and susceptibility (bottom) at  $T=2$  mK,  $H \parallel (001)$ . A  $5 \times 5 \times 5$  model has been used to generate these data. Open and solid symbols represent the data for the model which included nearest-neighbor exchange interaction with and without dipolar forces respectively.

to the appearance of a collinear long-range ordered state induced by an applied magnetic field. In complete agreement with the theory,<sup>31</sup> which analyzes an order by disorder mechanism in various highly frustrated antiferromagnets, an ordering happens only around a special value of the magnetic field—one third of the saturation field in the case of a garnet lattice.

In GGG, that is, in a model which includes the dipolar forces, an ordered magnetic structure induced by an applied field is characterized by the appearance of a nonzero average value of the perpendicular component of local magnetization. The field dependence of parallel and perpendicular components of local magnetization at constant temperature is shown on Fig. 7, while Fig. 8 shows its temperature dependence in constant field. The two sets of curves on each of these figures reflect the fact that in applied magnetic field the 24 Gd sites are split unequally into two different symmetry sites—A and B sites in the notation of Ref. 21. When the field is applied along the  $(001)$  direction, the 8 A sites (represented by solid symbols on Figs. 7 and 8) are of higher symmetry than the 16 B sites (represented by open symbols). Clearly,  $\langle M \rangle_{xy}$  on the A sites serves as an order parameter for the transition from a paramagnetic state into an antiferromagnetically ordered state. Spins on the B sites, however, retain a nonzero value of the perpendicular component of magnetization even in the paramagnetic state. This effect is caused by the dipole-dipole interaction.

In order to avoid problems with possibly many metastable states the calculations were always started at high temperatures and fields and then the system annealed as it came into equilibrium at the desired field and temperature for measurement. However, even taking these precautions the problem of long equilibration times at low-temperature low-field region was unavoidable. Therefore an abrupt jump of magnetization around  $H=0.25$  T clearly visible on Fig. 7 is most likely to be an artificial result.

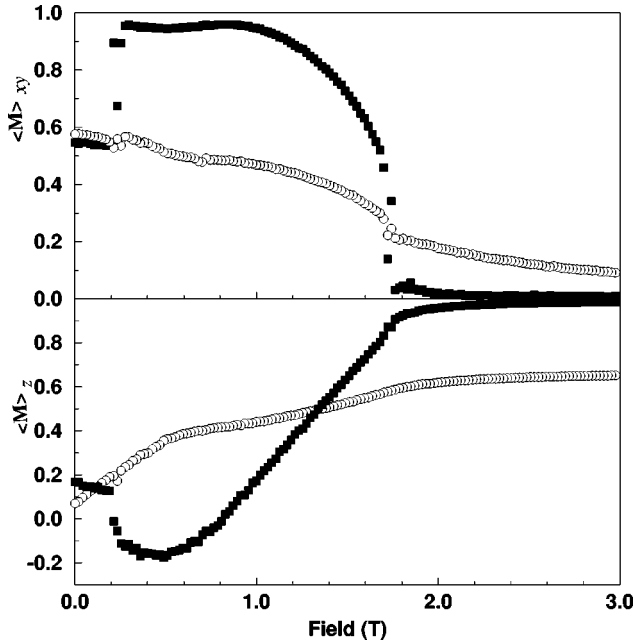


FIG. 7. Field dependence of parallel (bottom) and perpendicular (top) component of local magnetization at  $T=0.1$  K,  $H\parallel(001)$ . For notation see main text.

Even without detailed knowledge of the magnetic structure in a field we can check how stable it is to the introduction of second and third next to nearest exchange interactions,  $J_2$  and  $J_3$ . This has been done by calculating the neutron scattering function  $S_p(Q)$  for a  $3 \times 3 \times 3$  system according to formula (2). The results suggest that the magnetic order is rather stable in all four quadrants in the  $J_2$ - $J_3$  plane. The structure does not change when  $J_2 = -0.003$  K and  $J_3 = 0.010$  K are introduced corresponding to the values quoted in Ref. 20.

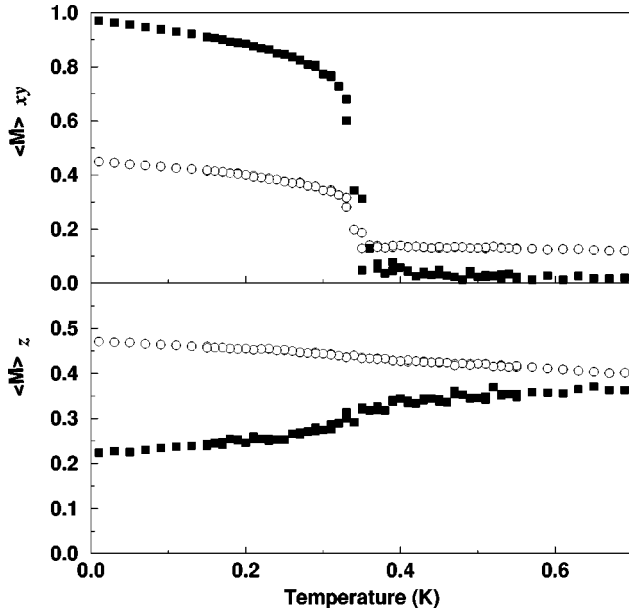


FIG. 8. Temperature dependence of parallel (bottom) and perpendicular (top) component of local magnetization in a field  $H=1.06$  T,  $H\parallel(001)$ . For notation see main text.

In an applied magnetic field, where LRO is developed, the formula (2) is no longer valid. Although it unambiguously shows the appearance of magnetic Bragg peaks, their intensity is not calculated correctly. However the overall field dependence of the intensity mimics extremely well the experimental data.<sup>19</sup> There are two different groups of magnetic peaks, ferromagnetic and antiferromagnetic. The intensity of the former group is growing in lower fields and saturating in a higher field. The intensity of the latter group also grows in lower fields reaching a maximum at around  $H=1$  T and then decreases in higher fields and disappears above  $H=2$  T. Exactly the same behavior has been seen by simulating single-crystal scattering intensity according to formula (3). Bottom panel of Fig. 5 shows the results of such calculations for  $H=1.06$  T and  $T=200$  mK. In an applied magnetic field a set of strong and sharp Bragg peaks replaces diffuse magnetic scattering observed in zero field. One interesting aspect of the calculations must be emphasized here: the relative intensity of the symmetry related antiferromagnetic peaks, such as, for example, (210) and (120), is not constant in time. The intensity of each peak may change arbitrarily at any time from almost zero up to maximum value, while the sum of two peaks intensities remains constant.

The only discrepancy between the Monte Carlo results and the neutron scattering data in magnetic field is the presence in the latter of an incommensurate peak located between two antiferromagnetic peaks (200) and (210). While this incommensurate peak is clearly visible in the neutron scattering data,<sup>19</sup> neither  $S_p(Q)$  nor  $S_{xt}(Q)$  [including a model where the magnetic field is applied along the (110) and (111) directions] demonstrates peaks at an incommensurate position. The reason for the discrepancy remains unknown at the moment.

#### IV. CONCLUSIONS

To summarize, we have presented the results of classical Monte Carlo simulations for the low-temperature behavior of the frustrated antiferromagnet on a garnet lattice. We have studied several different models, paying particular attention to two of them. The first model, which includes only nearest-neighbor exchange interactions, does not order down to lowest temperature, neither does it show any signs of spin freezing. Calculations of the zero-temperature specific heat for such a model suggest the presence of soft modes. The indications of the phase transition into an ordered (presumably collinear) state have been found at low temperature in applied magnetic field around a third of the saturation field. The experimentally measured properties of GGG including the  $H$  vs  $T$  magnetic phase diagram are consistent with our findings for the simulation model which includes nearest-neighbor exchange interactions and also dipolar forces. A perpendicular component of local magnetization serves as an order parameter for the phase transition in an applied field.

In conclusion we discuss several questions, which have been considered in this article, but which most certainly require further theoretical investigations.

First, both the low-temperature specific heat  $C(T=0)$  and

the single crystal scattering function  $S_{xt}(Q)$  are unusually sensitive to the boundary conditions. The influence of particular boundary conditions on the appearance of soft modes and incommensurate peaks in  $S_{xt}(Q)$  needs to be examined further.

Secondly, in the ordered state only the total intensity for the pairs of a symmetry related antiferromagnetic Bragg peaks, remains constant, while the intensity of an individual peaks may change. Could this behavior be related to the energy-free motion of long chains of magnetic moments,

similar to what happens in the *kagomé* lattice, or is it a sign of the domain walls movement?

#### ACKNOWLEDGMENTS

We are grateful to J. T. Chalker, M. J. P. Gingras, M. J. Harris, C. L. Henley, P. C. Holdsworth, R. Moessner, and M. E. Zhitomirsky for discussions and other valuable contributions and also to J. N. Reimers for his help with the computer calculations on the initial stages of the project.

- <sup>1</sup>B. Canals and C. Lacroix, Phys. Rev. Lett. **80**, 2933 (1998); R. Moessner, Phys. Rev. B **57**, R5587 (1998); R. Moessner and A.J. Berlinsky, Phys. Rev. Lett. **83**, 3293 (1999); E.H. Lieb and P. Schupp, *ibid.* **83**, 5362 (1999).
- <sup>2</sup>J.T. Chalker and J.F.G. Eastmond, Phys. Rev. B **46**, 14 201 (1992); P. Azaria, C. Hooley, P. Lecheminant, C. Lhuillier, and A.M. Tsvelik, Phys. Rev. Lett. **81**, 1694 (1998); D.A. Garanin and B. Canals, Phys. Rev. B **59**, 443 (1999); S.K. Pati and R.R.P. Singh, *ibid.* **60**, 7695 (1999); P. Sindzingre, G. Misguich, C. Lhuillier, B. Bernu, L. Pierce, C. Waldtmann, and H.U. Everts, *ibid.* **84**, 2953 (2000); R. Shankar and D. Shubashree, Phys. Rev. B **61**, 12 126 (2000); R. Moessner, S.L. Sondhi, and P. Chandra, Phys. Rev. Lett. **84**, 4457 (2000).
- <sup>3</sup>M.J. Harris, S.T. Bramwell, P.C. Holdsworth, and J.D.M. Champion, Phys. Rev. Lett. **81**, 4496 (1998); S.T. Bramwell and M.J. Harris, J. Phys.: Condens. Matter **10**, L215 (1998); R. Moessner and J.T. Chalker, Phys. Rev. Lett. **80**, 2929 (1998).
- <sup>4</sup>R. Siddharthan, B.S. Shastry, A.P. Ramirez, A. Hayashi, R.J. Cava, and S. Rosenkranz, Phys. Rev. Lett. **83**, 1854 (1999).
- <sup>5</sup>Y. Kobayashi, T. Takagi, and M. Mekata, J. Phys. Soc. Jpn. **67**, 3906 (1998).
- <sup>6</sup>J.T. Chalker, P.C. Holdsworth, and E.F. Shender, Phys. Rev. Lett. **68**, 855 (1992).
- <sup>7</sup>H. Kawamura, Phys. Rev. Lett. **80**, 5421 (1998).
- <sup>8</sup>R. Moessner and J.T. Chalker, Phys. Rev. B **58**, 12 049 (1998).
- <sup>9</sup>B.D. Gaulin, in *Magnetic Systems with Competing Interactions*, edited by H. T. Diep (World Scientific, Singapore, 1994), p. 286; A.P. Ramirez, A. Hayashi, R.J. Cava, R. Siddharthan, and B.S. Shastry, Nature (London) **399**, 333 (1999); J.H. Zhao, H.P. Kunkel, X.Z. Zhou, and G. Williams, Phys. Rev. Lett. **83**, 219 (1999); N.P. Raju, M. Dion, M.J.P. Gingras, T.E. Mason, and J.E. Greedan, Phys. Rev. B **59**, 14 489 (1999); M.J.P. Gingras, C.V. Stager, N.P. Raju, B.D. Gaulin, and J.E. Greedan, Phys. Rev. Lett. **78**, 947 (1997); M.J. Harris, S.T. Bramwell, D.F. McMorrow, T. Zeiske, and K.W. Godfrey, *ibid.* **79**, 2554 (1997); M.J. Harris, M.P. Zinkin, Z. Tun, B.M. Wanklyn, and I.P. Swainson, *ibid.* **73**, 189 (1994).
- <sup>10</sup>G. Balakrishnan, O.A. Petrenko, M.R. Lees, and D. McK Paul, J. Phys.: Condens. Matter **10**, L723 (1998).
- <sup>11</sup>A. Keren, P. Mendels, M. Horvatic, F. Ferrer, Y.J. Uemura, M. Mekata, and T. Asano, Phys. Rev. B **57**, 10 745 (1998); C. Mondelli, K. Andersen, H. Mutka, C. Payen, and B. Frick, Physica B **268**, 139 (1999); A. Keren, Y.J. Uemura, G. Luke, P. Mendels, M. Mekata, and T. Asano, Phys. Rev. Lett. **84**, 3450 (2000); A.P. Ramirez, B. Hessen, and M. Winklemann, *ibid.* **84**, 2957 (2000).
- <sup>12</sup>A. Harrison, A.S. Wills, and C. Ritter, Physica B **241-243**, 722 (1998); A.S. Wills, A. Harrison, S.A.M. Mentink, T.E. Mason, and Z. Tun, Europhys. Lett. **42**, 325 (1998); G.S. Oakley, D. Visser, J. Frunzke, K.H. Andersen, A.S. Wills, and A. Harrison, Physica B **268**, 142 (1999); G.S. Oakley, S. Pouget, A. Harrison, J. Frunzke, and D. Visser, *ibid.* **268**, 145 (1999); T. Inami, M. Nishiyama, S. Maegawa, and Y. Oka, Phys. Rev. B **61**, 12 181 (2000); A.S. Wills, A. Harrison, C. Ritter, and R.I. Smith, *ibid.* **61**, 6156 (2000).
- <sup>13</sup>S. Okubo, M. Hayashi, S. Kimura, H. Ohta, M. Motokawa, H. Kikuchi, and H. Nagasawa, Physica B **246**, 553 (1988); T. Fukamachi, Y. Kobayashi, A. Nakamura, H. Harashina, and M. Sato, J. Phys. Soc. Jpn. **68**, 3668 (1999).
- <sup>14</sup>J. Overmeyer, E.A. Giess, M.J. Freiser, and B.A. Calhoun, *Paramagnetic Resonance I*, edited by W. Low (Academic, New York, 1964), p. 224.
- <sup>15</sup>A.P. Ramirez and R.N. Kleiman, J. Appl. Phys. **69**, 5252 (1991).
- <sup>16</sup>J. Filippi, J.C. Lasjaunias, A. Ravex, F. Tcheou, and J. Rossat-Mignod, Solid State Commun. **23**, 613 (1977); D.G. Onn, H. Meyer, and J.P. Remeika, Phys. Rev. **156**, 663 (1967).
- <sup>17</sup>W. Prandl, Phys. Status Solidi B **55**, K159 (1973); A. Gukasov, V.P. Plakhty, B. Dorner, S.Yu. Kokovin, V.N. Syromyatnikov, O.P. Smirnov, and Yu.P. Cherenkov, J. Phys.: Condens. Matter **11**, 2869 (1999).
- <sup>18</sup>O.A. Petrenko, C. Ritter, M. Yethiraj, and D. McK Paul, Phys. Rev. Lett. **80**, 4570 (1998).
- <sup>19</sup>O.A. Petrenko, D. McK Paul, C. Ritter, T. Zeiske, and M. Yethiraj, Physica B **266**, 41 (1999).
- <sup>20</sup>W.I. Kinney and W.P. Wolf, J. Appl. Phys. **50**, 2115 (1979).
- <sup>21</sup>P. Schiffer, A.P. Ramirez, D.A. Huse, and A.J. Valentino, Phys. Rev. Lett. **73**, 2500 (1994).
- <sup>22</sup>R.A. Fisher, G.E. Brodale, E.W. Hornung, and W.F. Giauque, J. Chem. Phys. **59**, 4652 (1973).
- <sup>23</sup>A.B. MacIsaac, J.P. Whitehead, M.C. Robinson, and K. De'Bell, Phys. Rev. B **51**, 16 033 (1998).
- <sup>24</sup>B.C. den Hertog and M.J.P. Gingras, Phys. Rev. Lett. **84**, 3430 (2000).
- <sup>25</sup>J.N. Reimers, Phys. Rev. B **45**, 7287 (1992).
- <sup>26</sup>P. Schiffer, A.P. Ramirez, D.A. Huse, P.L. Gammel, U. Yaron, D.J. Bishop, and A.J. Valentino, Phys. Rev. Lett. **74**, 2379 (1995).
- <sup>27</sup>J. Villain, Z. Phys. B: Condens. Matter **33**, 31 (1979).



<sup>28</sup>R.N. Bhatt and A.P. Young, Phys. Rev. Lett. **54**, 924 (1985).

<sup>29</sup>O.A. Petrenko and D. McK Paul, AIP Conf. Proc. No. 479 (AIP, Woodbury, NY, 1999), p. 90.

<sup>30</sup>T.V. Valyanskaya, V.P. Plakhtii, and V.I. Sokolov, Zh.

Eksp. Teor. Fiz. **70**, 2279 (1976) [Sov. Phys. JETP **43**, 1189 (1976)].

<sup>31</sup>M.E. Zhitomirsky, A. Honecker, and O.A. Petrenko, Phys. Rev. Lett. **85**, 3269 (2000).